

## Article

# Development of Pure Silica CHA Membranes for CO<sub>2</sub> Separation

Gabriel Gama da Silva Figueiredo <sup>1</sup>, Daishi Takayama <sup>1</sup>, Katsunori Ishii <sup>1</sup>, Mikihiro Nomura <sup>1,\*</sup>, Takamasa Onoki <sup>2</sup>, Takuya Okuno <sup>2</sup>, Hiromasa Tawarayama <sup>2</sup> and Shinji Ishikawa <sup>2</sup>

<sup>1</sup> Shibaura Institute of Technology, 3-7-5 Toyosu, Koto-ku, Tokyo 135-8548, Japan; mc20501@shibaura-it.ac.jp (G.G.d.S.F.); mc19008@shibaura-it.ac.jp (D.T.); na19101@shibaura-it.ac.jp (K.I.)

<sup>2</sup> Sumitomo Electric Industries Ltd., 1 Taya-cho, Sakae-ku, Yokohama 244-8588, Japan; onoki-takamasa@sei.co.jp (T.O.); okuno-takuya@sei.co.jp (T.O.); tawarayama-hiromasa@sei-co.jp (H.T.); ishishin@sei.co.jp (S.I.)

\* Correspondence: Lscathy@shibaura-it.ac.jp

**Abstract:** Thin pure-silica chabazite (Si-CHA) membranes have been synthesized by using a secondary growth method on a porous silica substrate. A CO<sub>2</sub> permeance of  $2.62 \times 10^{-6} \text{ mol m}^{-2} \text{ s}^{-1} \text{ Pa}^{-1}$  with a CO<sub>2</sub>/CH<sub>4</sub> permeance ratio of 62 was obtained through a Si-CHA membrane crystallized for 8 h using a parent gel of H<sub>2</sub>O/SiO<sub>2</sub> ratio of 4.6. The CO<sub>2</sub> permeance through the Si-CHA membrane on a porous silica substrate was twice as high as that through the membrane synthesized on a porous alumina substrate, which displayed a similar zeolite layer thickness.

**Keywords:** membrane separation; inorganic membrane; zeolite; pure silica CHA-type zeolite; CO<sub>2</sub> separation; silica substrates



**Citation:** Figueiredo, G.G.d.S.; Takayama, D.; Ishii, K.; Nomura, M.; Onoki, T.; Okuno, T.; Tawarayama, H.; Ishikawa, S. Development of Pure Silica CHA Membranes for CO<sub>2</sub> Separation. *Membranes* **2021**, *11*, 926. <https://doi.org/10.3390/membranes11120926>

Academic Editors: Pei Sean Goh, Takeshi Matsuura and Mohd Hafiz Dzarfan Othman

Received: 31 October 2021  
Accepted: 23 November 2021  
Published: 25 November 2021

**Publisher's Note:** MDPI stays neutral with regard to jurisdictional claims in published maps and institutional affiliations.



**Copyright:** © 2021 by the authors. Licensee MDPI, Basel, Switzerland. This article is an open access article distributed under the terms and conditions of the Creative Commons Attribution (CC BY) license (<https://creativecommons.org/licenses/by/4.0/>).

## 1. Introduction

The development of efficient and sustainable CO<sub>2</sub> capture technologies is desired for several reasons. First, carbon dioxide is a common greenhouse gas found in combustion streams. In other words, its production is present in many industrial processes, and its accumulation in the atmosphere is a threat to many bio systems on the planet [1]. Additionally, CO<sub>2</sub> is one of the main components of raw natural gas, and is responsible for pipeline corrosion problems during gas transportation [2]. For these reasons, separation technologies for carbon capture and storage (CCS) have been developed, such as pressure swing adsorption, amine scrubbing, and cryogenic distillation [3,4]. Among these separation techniques, membrane separation has presented itself as one of the most efficient methods, thus receiving increasing attention from the scientific community [5]. Fard et al. [6] reported that the global demand for membranes and membrane modules reached 15.6 billion USD in 2018, and is expected to grow annually by 8%.

Membranes are usually classified into 2 broad classes: polymeric and inorganic membranes. Although losing in terms of reproducibility, inorganic membranes are known for displaying superior thermal, chemical and mechanical stabilities when compared with polymeric membranes [7,8]. Therefore, inorganic membranes are preferentially applied for high temperature gas separation processes [9,10]. Among the materials used for the fabrication of inorganic membranes, zeolites excel as adsorbents due to their narrow and uniform pore size, high surface area, adjustable hydrophilicity and hydrophobicity, ion exchange capacity, and strong acidity [11]. In particular, chabazite (also known as CHA-type zeolite) has been researched for CO<sub>2</sub> separation, due to its eight-membered ring pores of 0.38 nm. For that reason, since the molecular diameters of CO<sub>2</sub> and CH<sub>4</sub> are 0.33 nm and 0.38 nm, respectively, CHA membranes show high CO<sub>2</sub>/CH<sub>4</sub> selectivity [12,13]. Kida et al. [14] reported that a CHA membrane synthesized on an alumina substrate without adding aluminum in the parent gel showed a CO<sub>2</sub>/CH<sub>4</sub> selectivity of 130, with a CO<sub>2</sub> permeance

of  $4.0 \times 10^{-6} \text{ mol m}^{-2} \text{ s}^{-1} \text{ Pa}^{-1}$ . Yu et al. [15] synthesized an industrially relevant CHA membrane, with a length of 50 cm and membrane area of  $100 \text{ cm}^2$ , which displayed a  $\text{CO}_2$  permeance of  $1.6 \times 10^{-6} \text{ mol m}^{-2} \text{ s}^{-1} \text{ Pa}^{-1}$  and a  $\text{CO}_2/\text{CH}_4$  selectivity as high as 236. Hasegawa et al. [16] prepared a high silica CHA-type zeolite membrane ( $\text{Si}/\text{Al} = 18$ ) on a porous  $\alpha\text{-Al}_2\text{O}_3$  substrate with  $\text{N}_2/\text{SF}_6$  and  $\text{CO}_2/\text{CH}_4$  selectivities of 710 and 240, respectively. These high separation performances were explained by the low concentration or absence of aluminum in the parent gels during the synthesis of the CHA membrane. In the zeolite structure, cations are adhered to the negatively charged aluminum sites, which in turn increase the diffusion resistance of  $\text{CO}_2$  in the zeolite pores. Therefore, the preparation of pure silica CHA (Si-CHA) membranes is expected to increase  $\text{CO}_2$  separation performances. However, the highest achievable Si/Al ratio of CHA crystals in the conventional hydroxide medium is lower than 100 due to competition with other zeolites, such as ITQ-1, SSZ-23, and SSZ-24 [17]. For the parent gels that do not contain aluminum in its composition, CHA membranes have been prepared in fluoride medium, with rather low  $\text{H}_2\text{O}/\text{SiO}_2$  ratios of 3–6 in order to obtain a successful crystallization [17–19]. Only a few research groups were able to synthesize high silica membranes with parent gels of higher  $\text{H}_2\text{O}/\text{SiO}_2$  ratios. For example, Zhou et al. [20] were able to synthesize a high silica CHA zeolite membrane with a  $\text{CO}_2/\text{CH}_4$  selectivity of 480 by using a fluoride and aluminum free parent gel with a  $\text{H}_2\text{O}/\text{SiO}_2$  ratio of 120.

Si-CHA membranes are usually synthesized on porous alumina substrates in order to increase the mechanical strength of the thin CHA separation layers. However, alumina substrates are dissolved in CHA parent gels due to their alkalinity [21–24]. One of the solutions to overcome the aluminum dissolution of the porous ceramic substrates is to instead synthesize the membrane on a porous silica substrate without aluminum in its structure. The effects of using porous silica substrates to improve gas permeance were investigated in the preparation of MFI membranes [25–27]. Sugiyama et al. [26] were able to obtain a  $\text{N}_2$  permeance through a MFI membrane of  $3.7 \times 10^{-6} \text{ mol m}^{-2} \text{ s}^{-1} \text{ Pa}^{-1}$  with a  $\text{N}_2/\text{SF}_6$  permeance ratio of 328. The application of porous silica substrates was effective for MFI membranes.

Therefore, in this paper, Si-CHA membranes were crystallized on porous silica substrates. The effects of changing the synthesis conditions were investigated for dense Si-CHA membranes for  $\text{CO}_2$  separation. Among these synthesis conditions, the effect of adding seed crystals to the synthesis gel was studied as well. Seeding is one of most important parameters for zeolite synthesis [28]. Kong et al. [17] reported that the presence of seed crystals favors the formation of CHA zeolite more than the presence of the structure directing agent (SDA). Finally, the effects of synthesizing the Si-CHA membrane on a silica substrate were confirmed by comparing the permeation results with those through a membrane synthesized on an alumina substrate.

## 2. Materials and Methods

### 2.1. Synthesis of Si-CHA Crystals

The Si-CHA crystals were synthesized by hydrothermal synthesis based on the former literature [12]. N,N,N-trimethyl-1-adamantylammonium hydroxide (TMAdaOH: 25%, SACHEM) was selected as the structure directing agent (SDA), and Tetraethyl orthosilicate (TEOS: >99%, LS-2430, Shin-Etsu) as the silica precursor. Both compounds were mixed and stirred at 250 rpm overnight, followed by heating until obtaining a dry powder. Then, hydrofluoric acid (HF: 46.0–48.0%, Wako) and distilled water were added to the dried powder to obtain the parent gel. The composition of the parent gel was  $\text{SiO}_2\text{:TMAdaOH:HF:H}_2\text{O} = 1\text{:}0.8\text{:}0.8\text{:}4.6$  (mol/mol). This dried gel was transferred to a PTFE-lined autoclave, where hydrothermal synthesis was carried out at  $150 \text{ }^\circ\text{C}$  for 24 h. The obtained CHA crystals were recovered by vacuum filtration and washed with distilled water. Then, after drying for 24 h, they were pulverized with an automatic mortar for 4 h. Finally, the CHA crystals were calcined in air at  $600 \text{ }^\circ\text{C}$  for 15 h in order to remove the SDA.

## 2.2. Synthesis of Si-CHA Membranes

The Si-CHA zeolite membranes were synthesized on porous silica tubes provided by Sumitomo Electric Industries, Ltd. (Yokohama, Japan) (outer diameter: 10 mm, inner diameter: 6 mm, average pore size: 500 nm, length 30 mm). The silica substrates were coated with the Si-CHA crystals by the dip-coating method, with a Si-CHA seed crystal slurry of  $8 \text{ g L}^{-1}$  concentration and pH 2. The composition of the parent gel for the membrane synthesis was  $\text{SiO}_2:\text{TMAOH}:\text{HF}:\text{H}_2\text{O} = 1:0.8:0.8:3.8\text{--}5.4$  (mol/mol). Moreover,  $10 \mu\text{m}$  Si-CHA crystals were also added to the synthesis gel at varying quantities (0–0.25 wt%). Then, 28 g of the parent gel was smeared onto a seeded substrate, followed by hydrothermal synthesis at  $150 \text{ }^\circ\text{C}$  for 4 h to 16 h in a Teflon-lined autoclave. After the synthesis, calcination was performed in air at  $600 \text{ }^\circ\text{C}$  for 5 h.

In order to investigate the effects of the substrates, an alumina substrate (outer diameter: 12 mm, inner diameter: 8 mm, average pore size: 500 nm, length 30 mm, Noritake Co. (Nagoya, Japan)) was employed. The synthesis procedures were the same as those for the silica substrate.

## 2.3. Characterization

The obtained membranes were characterized by using an X-ray diffractometer (Rigaku (Tokyo, Japan)) from  $5$  to  $40^\circ$  for  $\text{CuK}\alpha$  radiation. The morphologies of the obtained crystals and membranes were observed using a VE-8800 scanning electron microscope (SEM, KEYENCE (Osaka, Japan)). The permeation performances were measured by single gas permeance tests using the probe gases  $\text{H}_2$ ,  $\text{CO}_2$ ,  $\text{N}_2$ ,  $\text{CH}_4$  and  $\text{SF}_6$  at room temperature. As typically done, the membrane was inserted in a stainless steel module and sealed with silicone O-rings. The selected gas was fed on the outer side of the membrane with a feed flow of  $200 \text{ mL/min}$  and, after permeating the membrane, flowed to a handmade bubble flowmeter, where the volumetric flow rate and, consequently, gas permeance were determined.

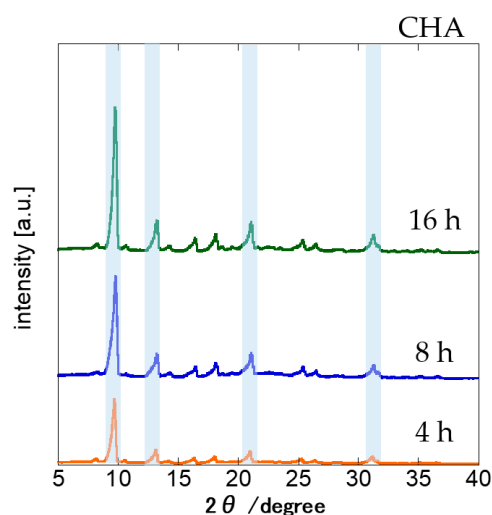
## 3. Results and Discussion

### 3.1. Effects of Synthesis Time

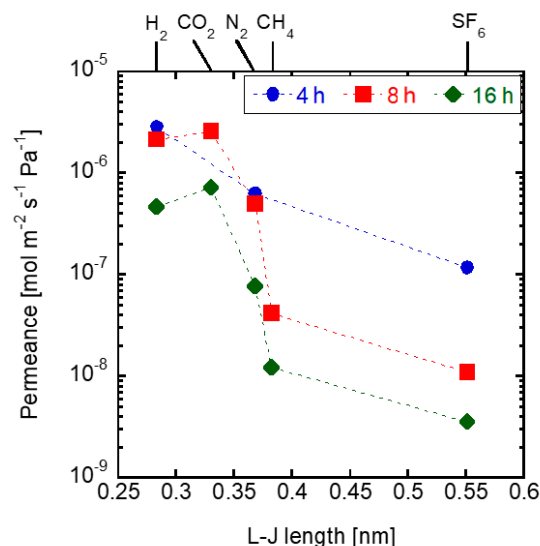
The synthesis time for the CHA zeolite membrane synthesis on the silica substrates was investigated from 4 h to 16 h at  $150 \text{ }^\circ\text{C}$ . The  $\text{H}_2\text{O}/\text{SiO}_2$  ratio and the added seed crystals were fixed at 4.6 and 0.01 wt%, respectively. Figure 1 shows the XRD patterns for the membranes. The highest diffraction peak at  $9.4^\circ$  refers to the (100) plane of the CHA and is considered its characteristic peak. All the other diffraction peaks were assigned for the CHA structure, with the exception of a very small peak at  $8.1^\circ$ . This peak was found in all membranes and refers to the (020) plane of the STT-type zeolite, a common impurity in CHA-type zeolite synthesis [18]. The obtained XRD peaks show that, starting from a synthesis time of 4 h, practically pure CHA layers were obtained, with the membrane synthesized for 16 h displaying, among the obtained membranes, the highest ratio of intensity of CHA and STT characteristic peaks. Specifically, a CHA ( $9.4^\circ$ )/STT ( $8.1^\circ$ ) of 25.3 was obtained, which is equivalent to about 96% Si-CHA purity. CHA ( $9.4^\circ$ )/STT ( $8.1^\circ$ ) ratios of 18 and 24 were obtained for the 4 h and 8 h synthesis, respectively. This shows that Si-CHA zeolite purity is proportional to synthesis time. The characteristic peak intensities at  $9.4^\circ$  increased by increasing the synthesis time. Therefore, the crystals' sizes are also proportional to the synthesis time.

Figure 2 shows the single gas permeances through the obtained membranes. The  $\text{H}_2/\text{SF}_6$  permeance ratio through the membrane synthesized for 4 h was 24.26. The Knudsen diffusion ratio of  $\text{H}_2/\text{SF}_6$  is 8.5, showing that the membrane synthesized for 4 h was not dense enough.  $\text{H}_2/\text{SF}_6$  permeance ratio through the membrane synthesized for 8 h was 196, which is much higher than that for 4 h synthesis. Furthermore, the membrane's  $\text{CO}_2$  permeance was of  $2.62 \times 10^{-6} \text{ mol m}^{-2} \text{ s}^{-1} \text{ Pa}^{-1}$ , with a  $\text{CO}_2/\text{CH}_4$  permeance ratio of 62. The membrane's high selectivity can be explained by the molecular sieve mechanism due to the pore size of the CHA structure. The high  $\text{CO}_2/\text{CH}_4$  permeance ratio indicates

that the membrane synthesized for 8 h was dense. The membrane synthesized for 16 h displayed a similar  $\text{CO}_2/\text{CH}_4$  permeance ratio of 60. Therefore, this membrane was also dense. However, its  $\text{CO}_2$  permeance was only  $7.32 \times 10^{-7} \text{ mol m}^{-2} \text{ s}^{-1} \text{ Pa}^{-1}$ , which is 71.2% lower than that through the 8 h synthesis membrane. The lower  $\text{CO}_2$  permeance can be explained by the thicker CHA layer after the 16 h synthesis. A similar result was obtained by Chew et al. [29], who synthesized on  $\alpha$ -alumina a membrane of SAPO-34, a type of zeolite with CHA structure, which displayed an ideal  $\text{CO}_2/\text{CH}_4$  selectivity of 56.



**Figure 1.** XRD measurements for the membranes crystallized for varying synthesis times (1  $\text{SiO}_2$ :0.8 TMAdaOH:0.8 HF:4.6  $\text{H}_2\text{O}$ , 0.01 wt% CHA seeds, at 423 K).



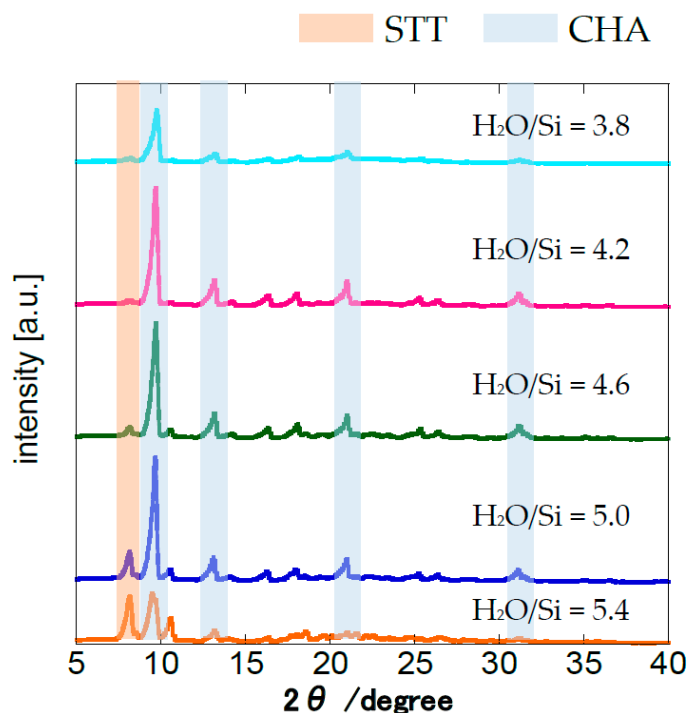
**Figure 2.** Single gas permeances through the membranes crystallized for varying synthesis times. (1  $\text{SiO}_2$ :0.8 TMAdaOH:0.8 HF:4.6  $\text{H}_2\text{O}$ , 0.01 wt% CHA seeds, at 423 K).

### 3.2. Effect of $\text{H}_2\text{O}/\text{SiO}_2$ Ratio of the Parent Gel

The effect of the  $\text{H}_2\text{O}/\text{SiO}_2$  ratio of the parent gel was investigated. The  $\text{H}_2\text{O}/\text{SiO}_2$  ratio varied from 3.8 to 5.4. The synthesis time was fixed at 16 h. The parent gel displayed a paste-like state. The viscosity of the parent gel is an important parameter, as the adherence of the paste to the surface of the substrate is necessary for the successful uniform synthesis of the zeolite layer.

Figure 3 shows the XRD patterns for the membranes crystallized with different  $\text{H}_2\text{O}/\text{SiO}_2$  ratios. The intensities at  $8.1^\circ$  increased when increasing the  $\text{H}_2\text{O}/\text{SiO}_2$  ra-

ratio of the parent gel. Miyamoto et al. [18] reported that synthesis gels with low  $\text{H}_2\text{O}/\text{SiO}_2$  ratios tend to initiate the formation of zeolites with lower framework densities. The framework densities of CHA and STT are  $15.4$  and  $17.0$   $\text{Si}/\text{nm}^3$ , respectively. Thus, the STT structure was more present in the surface of the membranes synthesized by the parent gels of lower silica concentration. A CHA ( $9.4^\circ$ )/STT ( $8.1^\circ$ ) intensity ratio of 29.5 was obtained when  $\text{H}_2\text{O}/\text{SiO}_2 = 4.2$ , the highest calculated from these XRD measurements. The CHA ( $9.4^\circ$ )/STT ( $8.1^\circ$ ) intensity ratio was only 13.8 when  $\text{H}_2\text{O}/\text{SiO}_2 = 3.8$  due to the low viscosity of the parent gel. Therefore, the gel's optimal  $\text{H}_2\text{O}/\text{SiO}_2$  ratio is 4.2, as it tends to produce a pure CHA layer, as well as displaying good viscosity.



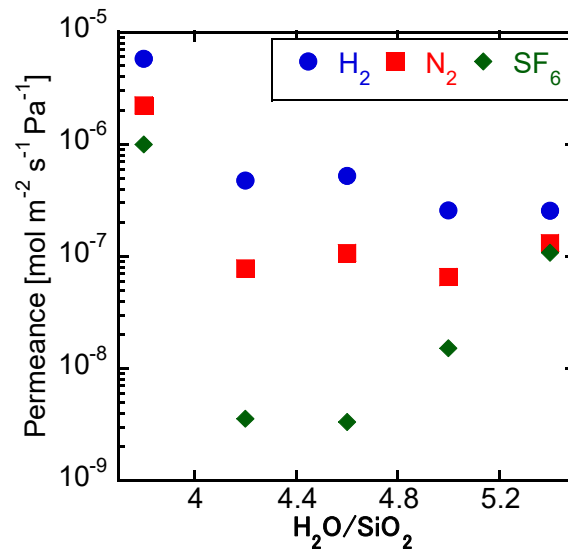
**Figure 3.** XRD measurements for the membranes crystallized with different  $\text{H}_2\text{O}/\text{SiO}_2$  ratios. (1  $\text{SiO}_2$ :0.8  $\text{TMAdaOH}$ :0.8  $\text{HF}$ :X  $\text{H}_2\text{O}$ , 0.01 wt% CHA seeds, 16 h at 423 K).

Figure 4 shows the single gas permeances through the membranes synthesized with different  $\text{H}_2\text{O}/\text{SiO}_2$  ratios. The overall high permeance of the membrane obtained with a parent gel of  $\text{H}_2\text{O}/\text{SiO}_2$  ratio of 3.8 was due to the low membrane thickness, consequent to the high viscosity of the parent gel. For this membrane, a low  $\text{H}_2/\text{SF}_6$  permeation ratio of 5.81 was obtained, due to the non-uniform coating of the parent gel on the substrate prior to crystallization. On the other hand, the  $\text{SF}_6$  permeance increased drastically when increasing the  $\text{H}_2\text{O}/\text{SiO}_2$  ratio to 5.0 and over. As a result, high  $\text{H}_2/\text{SF}_6$  permeance ratios over 130 were obtained only by the membranes with  $\text{H}_2\text{O}/\text{SiO}_2 = 4.2$  and 4.6. These membranes showed the highest CHA ( $9.4^\circ$ )/STT ( $8.1^\circ$ ) peak intensity ratios as well, displaying values of 29.5 and 25.3 for the membranes synthesized with the parent gels of  $\text{H}_2\text{O}/\text{SiO}_2$  ratios of 4.2 and 4.6, respectively. In order to obtain a uniform crystal layer, the STT phase in the CHA structure is not desirable.

### 3.3. Effect of Adding Seed Crystals to the Synthesis Gel

The amount of seed crystals in a parent gel of  $\text{H}_2\text{O}/\text{SiO}_2 = 4.6$  was investigated in a 16 h synthesis at  $150^\circ\text{C}$ . In these syntheses, the weight percentage of CHA seed crystals in the parent gel was varied from 0 to 0.25 wt%. Figure 5 shows the surface and the cross-sectional images of the SEM observation of the membranes. No CHA layer was observed in the case of the parent gel without any seed crystals. On the other hand, a polycrystalline structure was found in the membranes with 0.01 wt% and 0.05 wt% seed

crystals. The surface crystal size was of 1.07  $\mu\text{m}$  when 0.01 wt% seed crystals were added, while a smaller crystal size of 530 nm was obtained when 0.05 wt% seed crystals were added. Since the seed crystals in the parent gel function as crystallization nuclei, the number of CHA crystals should increase by increasing the amount of CHA seed crystals added to the parent gel [30,31]. Therefore, smaller crystals are obtained with higher amounts of seed crystals, since the total amount of zeolite is limited by the total amount of coated parent gel.



**Figure 4.** Single gas permeances through the membranes crystallized with varying H<sub>2</sub>O/SiO<sub>2</sub>. (1 SiO<sub>2</sub>:0.8 TMAdaOH:0.8 HF:X H<sub>2</sub>O, 0.01 wt% CHA seeds, 16 h at 423 K).

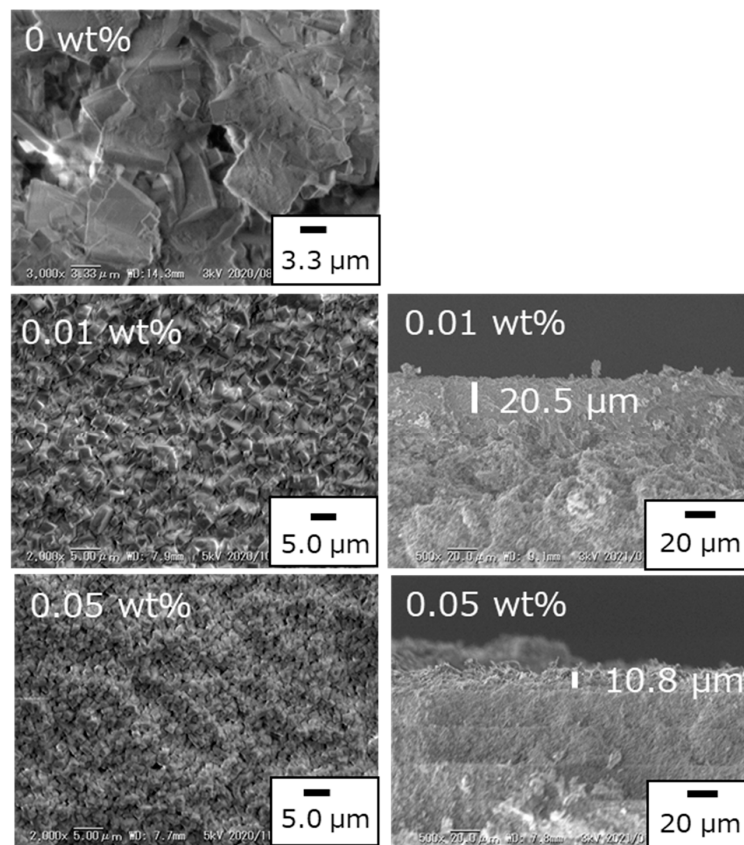


**Figure 5.** The effect on the morphology of pure silica CHA zeolite membranes by adding seed crystals (1 SiO<sub>2</sub>:0.8 TMAdaOH:0.8 HF:4.6 H<sub>2</sub>O, x wt% CHA seeds, 16 h at 423 K).

Figure 6 shows the single gas permeances through the membranes synthesized with different concentrations of seed crystals in the parent gel. The  $H_2/SF_6$  permeance ratio was of 2.37 in the case of the membrane synthesized with no addition of seed crystals. Additionally,  $H_2$  permeance was lower than that through the substrate. Judging by the low  $H_2/SF_6$  permeance ratio, it can be concluded that the membrane was not dense, as the molecular size of  $SF_6$  is larger than the pore size of CHA. However, both  $H_2/SF_6$  permeance ratio and  $H_2$  permeance increased with increasing the amounts of seed crystals in the parent gel. As discussed before, the crystal size decreased with increasing the amount of seed crystals in the parent gel, resulting in a thinner and denser CHA layer. However, the  $H_2/SF_6$  permeance ratio through the membrane prepared with the high seed crystal ratio of 0.25 wt% in the parent gel was only 16.88, lower than that through the membrane prepared with a seed crystal ratio of 0.05 wt%. The CHA layer must have been too thin to function as a dense membrane.

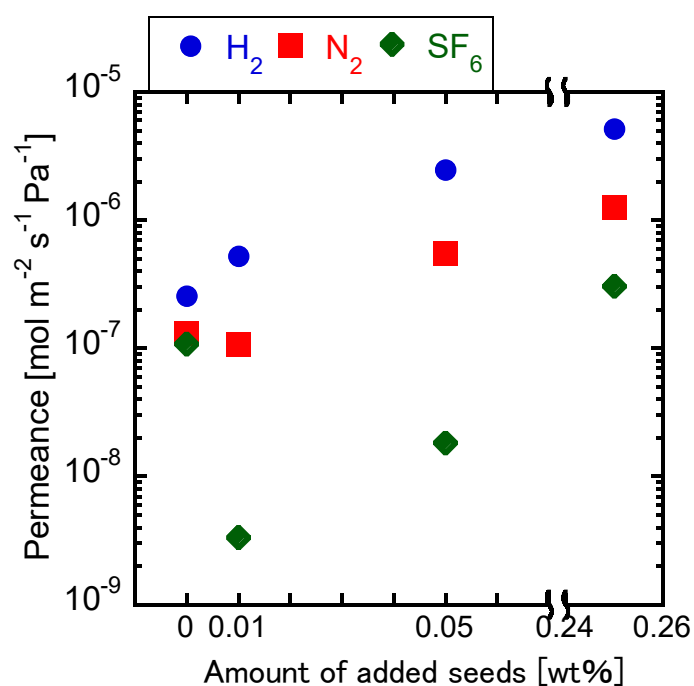


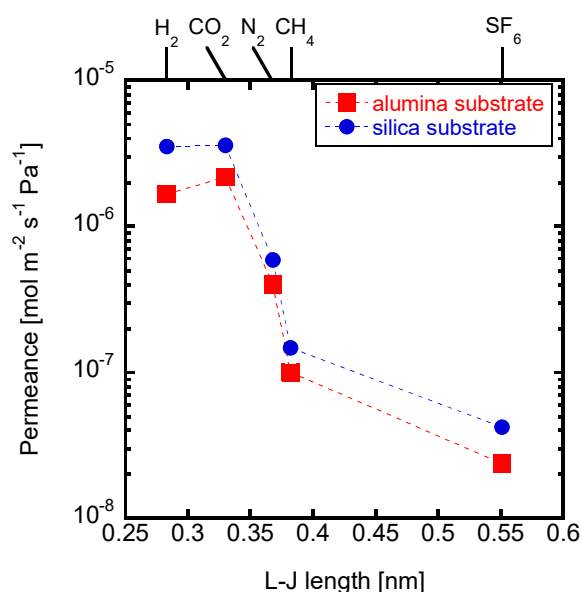
**Figure 6.** Single gas permeances through the membranes crystallized with varying seed crystal concentrations. (1  $\text{SiO}_2$ :0.8 TMAOH:0.8 HF:4.6  $\text{H}_2\text{O}$ , x wt% CHA seeds, 16 h at 423 K).

### 3.4. Effects of the Substrates

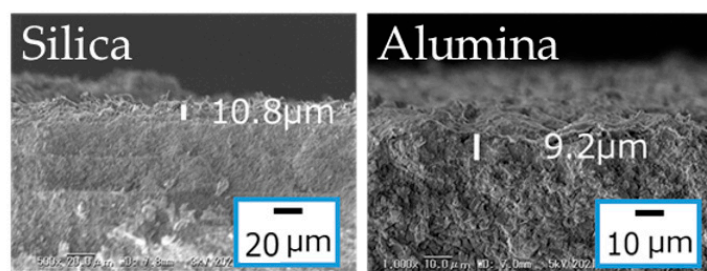
The synthesis procedure of the Si-CHA membrane on silica substrate was optimized in the former sections. In this section, a Si-CHA zeolite membrane was synthesized on an alumina substrate to confirm, by comparison, the effects of synthesizing a Si-CHA membrane on a silica substrate. Figure 7 shows the single gas permeances through the membranes synthesized on different types of substrates. Both membranes show similar  $H_2/SF_6$  permeance ratios of 71.05 (alumina) and 83.80 (silica). However, the  $H_2$  permeance through the membrane on the silica substrate was of  $3.53 \times 10^{-6} \text{ mol m}^{-2} \text{ s}^{-1} \text{ Pa}^{-1}$ , which is about twice as high than that through the membrane on the alumina substrate. Aluminum is dissolved from the alumina substrate during CHA synthesis, and the dissolved Al from the substrates can affect the Si/Al ratio of the CHA on the alumina substrate [26]. The membrane synthesized on alumina substrate has displayed a Si/Al ratio of about 5 by an X-ray spectroscopy (EDS) analysis. Cations are found around the Al atoms in the pores of the zeolite structure, and display a form of diffusion resistance [32]. However, this is not the case when synthesizing a zeolite membrane on a porous silica substrate. Therefore, CHA membranes with a Si/Al ratio of infinite can be synthesized on silica substrates to improve permeance.

Figure 8 shows the CHA zeolite layer thicknesses of the membranes synthesized on porous silica and alumina substrates. Both membranes displayed similar thicknesses of 10.8  $\mu\text{m}$  and 9.2  $\mu\text{m}$  for the membranes synthesized on silica and alumina substrates, respectively. The membrane synthesized on the alumina substrate was obtained with 170  $^{\circ}\text{C}$  and 70 h, whereas the one synthesized on the silica substrate was obtained with 150  $^{\circ}\text{C}$  and 16 h. Therefore, apart from the fact that Si-CHA membranes synthesized on porous silica substrates are more permeable than CHA membranes synthesized on alumina substrates, silica substrates also display a possibility of synthesizing CHA membranes on them with milder synthesis conditions.

Finally, both membranes have shown  $\text{CO}_2/\text{CH}_4$  separation potential, displaying  $\text{CO}_2/\text{CH}_4$  separation factors over 20.



**Figure 7.** Single gas permeances through the membranes crystallized on different types of substrates (1 SiO<sub>2</sub>:0.8 TMAdaOH:0.8 HF:4.6 H<sub>2</sub>O, 0.01 wt% CHA seeds, 16 h at 423 K).



**Figure 8.** Thicknesses of CHA zeolite membranes synthesized on different porous substrates. (1 SiO<sub>2</sub>:0.8 TMAdaOH:0.8 HF:4.6 H<sub>2</sub>O, x wt% CHA seeds, 16 h at 423 K).

#### 4. Conclusions

Si-CHA zeolite membranes were synthesized on novel silica substrates for the first time. The synthesis procedures were optimized to obtain a  $\text{CO}_2/\text{CH}_4$  selective membrane.

The membrane has displayed an increase of the separation layer thickness by increasing the synthesis time.  $\text{CO}_2/\text{CH}_4$  selectivity was slightly lower in the 16 h synthesis (59) when compared to the membrane synthesized for 8 h (62). However,  $\text{H}_2$  permeation was 71.2% lower in the case of the 16 h synthesis.

The synthesis gel should display an ideal concentration of water. If the water concentration is too low ( $\text{H}_2\text{O}/\text{SiO}_2 < 3.8$ ), the gel becomes too viscous. As a result, a zeolite layer displaying poor uniformity is obtained. On the other hand, a too high water concentration



( $\text{H}_2\text{O}/\text{SiO}_2 > 5$ ) results in the synthesis of STT zeolite. In this study, a water concentration of  $\text{H}_2\text{O}/\text{SiO}_2 = 4.2$  has resulted in the best uniformity of the zeolite layer among the studied range of  $\text{H}_2\text{O}/\text{SiO}_2$  ratio.

The concentration of Si-CHA seed crystals in the synthesis gel was investigated for the first time in this paper. The most prominent effect observed when adding seed crystals to the synthesis gel was the increase of the zeolite layer's density. The increased number of nuclei must have resulted in the synthesis of smaller Si-CHA crystals. The  $\text{H}_2/\text{SF}_6$  ideal selectivity was increased when 0.01–0.05 wt% of seed crystals were added to the synthesis gel.

Finally, regarding the choice of substrate, a clear effect in the overall gas permeance of the membranes was observed. It was possible to obtain an overall permeance twice as high as the same membrane synthesized on a porous alumina substrate by synthesizing the Si-CHA membrane on a silica porous substrate instead. By avoiding the effect of alumina dissolution from the substrate, pore blockage effect by ions and water can be averted.

The membrane with the highest  $\text{CO}_2/\text{CH}_4$  separation potential was synthesized on a porous silica substrate with the following conditions:  $\text{H}_2\text{O}/\text{SiO}_2$  ratio of 4.6 and addition of 0.01 wt% Si-CHA seed crystals in an 8 h synthesis at 150 °C. It is important to note that the synthesis of Si-CHA type zeolite membrane on porous silica substrates is still a novel technique, and still has much room for improvement.

**Author Contributions:** Conceptualization, M.N. and K.I.; methodology, D.T.; M.N. and K.I.; formal analysis, M.N. and K.I.; investigation, D.T.; resources, T.O. (Takamasa Onoki), T.O. (Takuya Okuno), H.T. and S.I.; data curation, M.N.; writing—original draft preparation, G.G.d.S.F.; writing—review and editing, M.N.; visualization, M.N.; supervision, M.N. and K.I.; project administration, M.N. and K.I. All authors have read and agreed to the published version of the manuscript.

**Funding:** This research received no external funding.

**Institutional Review Board Statement:** Not applicable.

**Data Availability Statement:** Not applicable.

**Conflicts of Interest:** The authors declare no conflict of interest.

## References

1. Whitfield, M. Accumulation of fossil  $\text{CO}_2$  in the atmosphere and in the sea. *Nature* **1974**, *247*, 523–525. [[CrossRef](#)]
2. Rufford, T.E.; Smart, S.; Watson, G.C.Y.; Graham, B.F.; Boxall, J.; Diniz da Costa, J.C.; May, E.F. The removal of  $\text{CO}_2$  and  $\text{N}_2$  from natural gas: A review of conventional and emerging process technologies. *J. Pet. Sci. Eng.* **2012**, *94–95*, 123–154. [[CrossRef](#)]
3. Behrooz, H.A.; Hoseini, M.; Mahamadzade, M.; Ranjbaran, N. Economic Comparison between Membrane and Adsorption Processes for Separation of  $\text{CO}_2$  and  $\text{CH}_4$  Mixture. In Proceedings of the 5th National Conference on New Researches in Chemistry and Chemical Engineering, Tehran, Iran, 4 February 2019.
4. Belaissaoui, B.; Moullec, Y.L.; Willson, D.; Favre, E. Hybrid membrane cryogenic process for post-combustion  $\text{CO}_2$  capture. *J. Memb. Sci.* **2012**, *415–416*, 424–434. [[CrossRef](#)]
5. Brunetti, A.; Macedonio, F.; Barbieri, G.; Drioli, E. Membrane engineering for environmental protection and sustainable industrial growth: Options for water and gas treatment. *Environ. Eng. Res.* **2015**, *20*, 307–328. [[CrossRef](#)]
6. Fard, A.K.; McKay, G.; Buekenhoudt, A.; Sulaiti, H.A.; Motmans, F.; Khraisheh, M.; Atieh, M. Inorganic Membranes: Preparation and Application for Water Treatment and Desalination. *Materials* **2018**, *11*, 74. [[CrossRef](#)] [[PubMed](#)]
7. Benfer, S.; Popp, U.; Richter, H.; Siewert, C.; Tomandl, G. Development and characterization of ceramic nanofiltration membranes. *Sep. Purif. Technol.* **2001**, *22–23*, 231–237. [[CrossRef](#)]
8. Nomura, M.; Yamaguchi, T.; Nakao, S. Silicalite Membranes Modified by Counter diffusion CVD Technique. *Ind. Eng. Chem. Res.* **1997**, *36*, 4217–4223. [[CrossRef](#)]
9. van Veen, H.M.; van Delft, Y.C.; Engelen, C.W.R.; Pex, P.P.A.C. Dewatering of organics by pervaporation with silica membranes. *Sep. Purif. Technol.* **2001**, *22–23*, 361–366. [[CrossRef](#)]
10. Songolzadeh, M.; Soleimani, M.; Ravanchi, M.T.; Songolzadeh, R. Carbon Dioxide Separation from Flue Gases: A Technological Review Emphasizing Reduction in Greenhouse Gas Emissions. *Sci. World J.* **2014**, *2014*, 828131. [[CrossRef](#)] [[PubMed](#)]
11. Miyamoto, M.; Fujioka, Y.; Yogo, K. Pure silica CHA type zeolite for  $\text{CO}_2$  separation using pressure swing adsorption at high pressure. *J. Mater. Chem.* **2012**, *22*, 20186. [[CrossRef](#)]
12. Kida, K.; Maeta, Y.; Yogo, K. Preparation and gas permeation properties on pure silica CHA-type zeolite membranes. *J. Memb. Sci.* **2017**, *522*, 363–370. [[CrossRef](#)]

13. Zhou, H.; Kean, W. The ‘ideal selectivity’ vs. ‘true selectivity’ for permeation of gas mixtures in nanoporous membranes. In *IOP Conference Series: Materials Science and Engineering*; IOP Publishing: Bristol, UK, 2018.
14. Kida, K.; Maeta, Y.; Yogo, K. Pure silica CHA-type zeolite membranes for dry and humidified CO<sub>2</sub>/CH<sub>4</sub> mixtures separation. *Sep. Purif. Technol.* **2018**, *197*, 116–121. [[CrossRef](#)]
15. Yu, L.; Nobandegani, M.S.; Hedlund, J. Industrially relevant CHA membranes for CO<sub>2</sub>/CH<sub>4</sub> separation. *J. Memb. Sci.* **2022**, *641*, 119888. [[CrossRef](#)]
16. Hasegawa, Y.; Abe, C.; Natsui, M.; Ikeda, A. Gas Permeation Properties of High-Silica CHA-Type Membrane. *Membranes* **2021**, *11*, 249. [[CrossRef](#)] [[PubMed](#)]
17. Kong, X.; Qiu, H.; Zhang, Y.; Tang, X.; Meng, D.; Yang, S.; Guo, W.; Xu, N.; Kong, L.; Zhang, Y.; et al. Seeded synthesis of all-silica CHA zeolites in diluted mother liquor. *Micro. Meso. Mater.* **2021**, *316*, 110914. [[CrossRef](#)]
18. Miyamoto, M.; Nakatani, T.; Fujioka, Y.; Yogo, K. Verified synthesis of pure silica CHA-type zeolite in fluoride media. *Micro. Meso. Mater.* **2015**, *206*, 67–74. [[CrossRef](#)]
19. Kim, E.; Cai, W.; Baik, H.; Choi, J. Uniform Si-CHA Zeolite Layers Formed by a Selective Sonication-Assisted Deposition Method. *Angew. Chem. Int. Ed.* **2013**, *52*, 5280–5284. [[CrossRef](#)]
20. Zhou, J.; Gao, F.; Sun, K.; Jin, X.; Zhang, Y.; Liu, B.; Zhou, R.; Benfer, S.; Popp, U.; Richter, H.; et al. Green Synthesis of highly CO<sub>2</sub>-selective CHA zeolite membranes in all-silica and fluoride-free solution for CO<sub>2</sub>/CH<sub>4</sub> separations. *Energy Fuels* **2020**, *34*, 11307–11314. [[CrossRef](#)]
21. Zarubin, D.P.; Nemkina, N.V. The solubility of amorphous silica in an alkaline aqueous medium at a constant ionic strength. *Russ. J. Inorg. Chem.* **1990**, *35*, 31–38.
22. Franke, M.D.; Ernst, W.R.; Myerson, A.S. Kinetics of dissolution of alumina in acidic solution. *Am. Inst. Chem. Eng.* **1987**, *33*, 267–273. [[CrossRef](#)]
23. Sano, T.; Yanagishita, H.; Kiyozumi, Y.; Mizukami, F.; Haraya, K. Separation of ethanol/water mixture by silicalite membrane on pervaporation. *J. Memb. Sci.* **1994**, *95*, 221–228. [[CrossRef](#)]
24. Eilertsen, E.A.; Milsen, M.H.; Wendelbo, R.; Olsbye, U.; Lillerud, K.P. Synthesis of high silica CHA zeolites with controlled Si/Al ratio. In *Proceedings of the 4th International FEZA Conference, Paris, France, 2–6 September 2008*; pp. 265–268.
25. Imasaka, S.; Nakai, A.; Araki, S.; Yamamoto, H. Synthesis and Gas Permeation of STT-type Zeolite Membranes. *J. Jpn. Pet. Inst.* **2018**, *61*, 263–271. [[CrossRef](#)]
26. Sugiyama, Y.; Ikarugi, S.; Oura, K.; Ikeda, A.; Matsuyama, E.; Ono, R.; Tawarayama, H.; Saito, T.; Kuwahara, K.; Nomura, M. MFI zeolite membranes prepared on novel silica substrates. *J. Chem. Eng. Jpn.* **2015**, *48*, 891–896. [[CrossRef](#)]
27. Tanizume, S.; Maehara, S.; Ishii, K.; Onoki, T.; Okuno, T.; Tawarayama, H.; Ishikawa, S.; Nomura, M. Reaction of methanol to olefin using a membrane contactor on a silica substrate. *Sep. Purif. Tech.* **2020**, *254*, 117647. [[CrossRef](#)]
28. Oleksiak, M.D.; Rimer, J.D. Synthesis of zeolites in the absence of organic structure-directing agents: Factors governing crystal selection and polymorphism. *Rev. Chem. Eng.* **2014**, *30*, 1–49. [[CrossRef](#)]
29. Chew, T.L.; Ahmad, A.L. Gas Permeation Properties of Modified SAPO-34 Zeolite Membranes. *Procedia Eng.* **2016**, *148*, 1225–1231. [[CrossRef](#)]
30. Grand, J.; Awala, H.; Mintova, S. Mechanism of zeolites crystal growth: New findings and open questions. *Cryst. Eng. Comm.* **2016**, *18*, 650–664. [[CrossRef](#)]
31. Nanev, C.N. Relationship between number and sizes of crystals growing in batch crystallization: Nuclei number density, nucleation kinetics and crystal polydispersity. *J. Cryst. Growth* **2020**, *546*, 125786. [[CrossRef](#)]
32. Drummond, D.; De Jonge, A.; Rees, L.V.C. Ion exchange kinetics in zeolite A. *J. Phys. Chem.* **1983**, *87*, 1967–1971. [[CrossRef](#)]